METHODOLOGY FOR QUANTITATIVE EVALUATION OF FLUID MUSCLES STIFFNESS IN SOFT ROBOTICS

MICHAL DUHANCIK[1], MARTIN KONDRAT[1], KAMIL ZIDEK[1], ALEXANDER HOSOVSKY[1], JAN PITEL[1], TIBOR KRENICKY[1], JOZEF HUSAR[1]

[1]Technical University of Kosice, Faculty of Manufacturing Technologies with seat in Presov, Bayerova 1, 080 01 Presov, Slovakia

DOI: 10.17973/MMSJ.2026_06_2026115

michal.duhancik@tuke.sk

The article presents an experimental methodology for evaluating fluid muscle stiffness using a controlled linear drive and a measuring chain based on a strain gauge force sensor. The measuring assembly consists of a strain gauge sensor, a signal converter, a programmable logic controller, and an electric actuator ensuring precise positioning. The measurements were performed at a vacuum level of 95% and at three extension lengths, i.e., muscle deflection from the base position (30, 60, and 90 mm), in order to test multiple load conditions. The results demonstrate a change in force response under vacuum loading and highlight the influence of granule rearrangement on stiffness variability at larger deformations. The proposed methodology ensures repeatability, diagnostic reliability, and suitability for characterizing soft robotics actuators, while also creating a robust experimental framework for the systematic evaluation of the stiffness characteristics of fluid muscles across a wide range of testing and loading conditions.

KEYWORDS

Soft robotics, Fluidic actuators, Force measurement, Stiffness measurement, PLC, Experimental methodology

1 INTRODUCTION

The historical context of stiffness measurement techniques is pivotal for understanding the evolution of methods used in assessing fluid continuous arms. Initially rooted in the fields of mechanical and civil engineering, early approaches primarily employed static and quasi-static measurements to determine material rigidity. As technologies advanced, the incorporation of dynamic analysis allowed for more nuanced evaluations, adapting practices from soft robotics and continuum mechanics to better model the complexities intrinsic to fluid dynamics. This shift reflects broader trends in the research community, where interdisciplinary approaches are increasingly utilized to address challenges in engineering applications, as highlighted in recent reviews focusing on nanophononics and metamaterials [Krushynska 2023].

The study of fluidic continuous arms has specifically changed the way we perceive and work with robotic systems in the rapidly developing field of soft robotics. Due to their flexibility and adaptability, fluid systems require sophisticated techniques to evaluate their mechanical properties, particularly stiffness, which is essential for effective operation. In order for these arms to be used practically in manufacturing, healthcare, and other areas where traditional rigid robots may not be suitable, it is essential to understand how to measure their stiffness.

The use of various theoretical frameworks and computational methods based on continuum mechanics and materials science is key to accurately capturing the behavior of these systems as their complexity increases [Armanini 2022]. In addition to improving our fundamental knowledge, research into fluid arms opens the door to innovative solutions, underscoring the need for thorough measurement techniques in the development of soft robotic technology [Jubelin 2022].

The concept of fluid continuous arms refers to flexible robotic structures that utilize fluid dynamics to achieve movement and functionality. Unlike traditional rigid arms, fluid continuous arms are composed of materials that can deform without breaking, allowing for enhanced maneuverability in complex environments. This characteristic is particularly beneficial in applications such as minimally invasive surgery, where navigation through tight spaces is crucial. Recent advancements in the field highlight the importance of modeling and control methods specifically designed for these continuum robots, as their unique biomechanics present challenges not found in conventional robotic systems [Russo 2023].

Recent studies suggest that improvements in measurement methods have a direct impact on the creation of increasingly complex continuum robots capable of performing advanced tasks in constrained environments, thus solving tasks that were previously unattainable in various fields [Russo 2023]. In addition, the quantification of stiffness is becoming key to accurately reproducing biomechanical behavior, which is important for drug response studies in cancer research, as fluid continuous arms increasingly integrate three-dimensional (3D) modeling methodologies [Jubelin 2022]. This systematic summary of measurement methods highlights the importance of making appropriate methodological decisions, as they directly affect the accuracy and usability of stiffness assessments. Furthermore, when examining bistable and multistable structures in soft actuator design, it highlights the importance of thoroughly understanding measurement methods, especially in the context of high-performance robotic applications [Chi 2022]. Therefore, the development of fluid arms in various technical applications depends on accurate stiffness measurement.

Stiffness, defined as the resistance of an object to deformation under applied force, can be influenced by various factors such as material properties, geometry, and boundary conditions. In fluidic systems, stiffness is not merely a function of material rigidity; it also depends on fluid density and the dynamic interplay between fluid pressure and structural elements. Bistable mechanisms, which exhibit distinct states of equilibrium, can offer enhanced performance in the design of such arms, allowing for rapid transitions and responsive adaptations in robotic applications [Chi 2022].

Stiffness measurements are critical in evaluating the performance of fluid continuous arms, as various factors significantly affect their accuracy and reliability.

One primary consideration is the material composition of the arms, wherein the use of advanced materials such as carbon nanotube-reinforced composites can enhance mechanical properties, thus influencing stiffness outcomes. The inherent properties of these materials, as detailed in [Mohd Nurazzi 2021], including their microstructure and functionalization techniques, play a pivotal role in determining stiffness. Additionally, the design and actuation method employed, particularly in applications utilizing pneumatic actuation, can impact stiffness measurements due to their dynamic responses to external forces [Xavier 2022]. Environmental conditions,

such as temperature and humidity, can also alter the stiffness of materials over time, further complicating precise measurements.

Therefore, understanding these factors is essential for improving accuracy in stiffness evaluations of fluid continuous arms. Researchers can alter the mechanical characteristics of these arms and evaluate their performance in both static and dynamic situations by utilizing a variety of actuation techniques. For example, using magnetism as an actuation mechanism shows great promise for improving the control and responsiveness of bioinspired microrobots in complex tasks [Ebrahimi 2020]. Additionally, the use of electronic skin technologies enhances the assessment procedure by enabling the measurement of tactile feedback and environmental interaction, both of which are critical for the efficient operation of robotics and prosthetics [Yang 2019]. In addition to clarifying the connection between fluid dynamics and mechanical stiffness, this analytical approach can help guide future design advancements and ensure that fluid continuous arms successfully meet application-specific requirements.

Among the various techniques employed, sensors such as strain gauges, pressure transducers, and accelerometers are instrumental in capturing real-time performance metrics under varying conditions. By utilizing these instruments, researchers can monitor the dynamic response of the fluid arms, offering insights into their mechanical properties. Moreover, computational modeling based on continuum mechanics is increasingly used to simulate the behavior of these systems, thereby supplementing experimental data with theoretical predictions. This synergy between empirical measurements and computational analysis enriches the understanding of stiffness characteristics, as noted in the overview of modeling approaches in soft robotics, which can guide future research efforts in this domain [Yang 2021].

Improvements in the measurement of fluid continuous arms' stiffness have important implications for research and industry, driving advances across multiple fields. As demonstrated by material jetting (MJ) technology, which is rapidly being adopted in biomedicine and aviation, the incorporation of accurate stiffness measurements can improve the manufacturing of high-dimensional accuracy components [Gulcan 2021]. The development of soft robotics in the agricultural sector, specifically in the design of soft grippers, depends on an understanding of material stiffness to ensure efficient handling of delicate products and enable automated harvesting solutions [Navas 2021]. The potential for increased productivity and product integrity across industries is highlighted by these intersections. Real-time monitoring using industrial devices enables the collection of process data that can help create a digital twin of the system in the future [Zidek 2024].

2 METHODOLOGY

Various measurement techniques are employed to quantify this stiffness, primarily focusing on dynamic and static methods. Dynamic techniques utilize oscillatory forces to assess the system's response, providing insights into both stiffness and damping characteristics. Conversely, static methods involve applying a controlled load and measuring the resultant deformation, yielding direct stiffness values. Recent advancements in technology have led to more sophisticated approaches, such as the development of electronic skins that can enhance tactile sensing capabilities, which are vital for real-time stiffness measurements in fluidic systems [Yang 2019]. Moreover, the intricate interplay between fluid dynamics and material properties necessitates a comprehensive understanding of the measuring environment, thus highlighting the importance of expert consensus in standardizing these measurement techniques for improved accuracy and reliability [Schneider 2021].

The assessment of stiffness in fluid continuous arms depends heavily on the integration of sophisticated sensors and instruments. These technical advancements make it possible to precisely analyze dynamic responses to changing loads, which is crucial for performance optimization in a variety of applications, including biomedical devices and robotics. Researchers can obtain an extensive collection of data on stress, strain, and deformation by using multifunctional sensor arrays. This enables a comprehensive assessment of material properties under practical conditions [Hasan 2024].

The measurement of stiffness in fluid continuous arms often results in a pivotal comparison between static and dynamic techniques, each offering distinct advantages and limitations. Static measurement techniques typically involve applying a constant load and measuring the resulting displacement, providing straightforward calculations of stiffness. However, these methods may not fully capture the inherent properties of soft robotic structures, which can exhibit time-dependent behaviors under varying conditions.

In contrast, dynamic measurement techniques involve subjecting the arm to oscillatory inputs, allowing for the assessment of stiffness in a manner that more accurately reflects real-world applications. This dynamic approach is particularly relevant in soft robotics, where materials often respond differently to varying loads [Armanini 2022]. Moreover, the ability of dynamic measurements to account for factors such as inertia and damping is crucial for comprehensive analysis, as identified in recent studies of soft pneumatic actuators and their applications [Xavier 2022].

This comparison highlights the necessity of selecting the appropriate measurement technique to ensure accurate representation of stiffness in fluid continuous arms. Additionally, the dynamic nature of fluid movements introduces complexities such as pressure fluctuations and fluid inertia, which can skew results. These factors necessitate a robust framework for modeling and characterization, incorporating advancements in data-driven methodologies and nonlinear control techniques. Ultimately, achieving accurate stiffness measurement is crucial, as it not only affects robotic performance but also influences design considerations for real-world applications, where precision and reliability are paramount [Yang 2021].

An essential component of assessing stiffness in fluidic continuous arms is the interpretation of experimental data, which gives scientists insight into the underlying mechanical characteristics that affect the material's behavior. Understanding how different elements, including surfactant interactions, affect flow dynamics and material properties is crucial for accurate analysis. Surfactants, for instance, have the power to dramatically change interfacial tension and affect how pressurized fluid-filled arms behave mechanically. According to current research, the way surfactants behave at interfaces might skew or complicate interpretation because various surfactant processes can produce comparable flow characteristics, which could cause results to be misinterpreted [Manikantan 2020].

Adopting a thorough strategy that combines fluid dynamics and thermodynamic concepts is crucial to addressing these problems, as it facilitates accurate stiffness measurements in these intricate systems and provides a clearer understanding of experimental data [Yang 2021].

3 MATERIAL AND METHODS

This chapter outlines the products and sensors used throughout the experimental trial, including those involved in data acquisition and processing. It describes the key technical characteristics of each component, along with its operating principles, in order to provide a clear understanding of the experimental setup and the methodological framework underlying the study.

3.1 Tensometric sensor

Strain gauge sensors convert mechanical deformation into an electrical signal proportional to the applied force, providing reliable and accurate measurements for both static and dynamic testing. Their small size facilitates smooth integration into experimental setups and industrial machinery. Such sensors are often used in research in the fields of materials testing, robotics, and biomechanics. They facilitate the quantification of tensile and compressive forces for characterizing material properties, analyzing contact forces in robotic systems, and investigating interaction forces in medical and biomechanical applications. Many scientific studies use strain gauge-based force sensors to quantify grip force, interaction forces between instruments and tissue in minimally invasive surgery, or small contact forces in precision assembly tests.

Measuring force during these processes ensures consistent quality and early detection of faulty components. A KD34S-10N (Fig. 1) strain gauge sensor with a nominal range of ±10 N was used to capture the forces involved. The output signal varies linearly with the excitation voltage applied to the bridge, meaning that its typical sensitivity is approximately 0.5 mV/V at nominal load. The accuracy class is approximately 0.1% of the full output range, which includes repeatability, hysteresis, and non-linearity. The sensor features a compact mechanical design (length of approximately 34 mm) and low weight, making it suitable for dynamic and space-constrained assemblies. The aluminum construction provides a good balance between stiffness, sensitivity, and thermal behavior [MeSystems 2026].

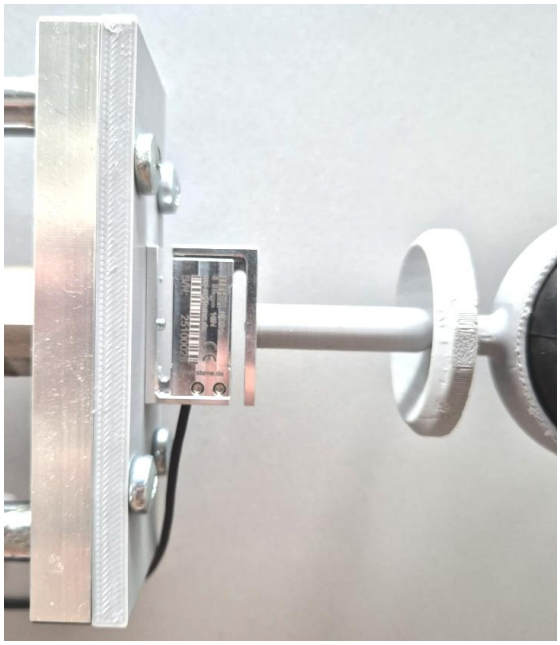

Figure 1. Tensometric sensor KD34S-10N

3.2 Converter

The EMS170 (Fig. 2) is a signal converter designed for strain gauge-based sensors that operate with a Wheatstone bridge. Since these sensors typically produce very small output signals in the mV/V range, the converter acts as an interface between the sensor and higher-level control or measurement systems. It amplifies and converts the weak bridge signal into standardized industrial outputs such as ±10 V or 4–20 mA, which can be processed by PLCs, data acquisition systems, or industrial controllers.

To ensure stable and reliable measurements in real-world applications, the EMS170 includes an active second-order low-pass filter. Selectable cutoff frequencies of 4 Hz, 40 Hz, or 400 Hz allow the signal bandwidth to be tailored to the measurement task. For slowly changing forces, such as in materials testing or pressure monitoring, lower filter settings (e.g., 4 Hz) help suppress electrical noise and mechanical vibrations. For faster processes, such as dynamic load measurement or impact detection, higher cutoff frequencies (40 Hz or 400 Hz) preserve more signal dynamics [EMSYST 2025].

Typical applications include monitoring assembly forces, quality control in joining processes, long-term load measurements in structural testing, and experimental research where clean and stable force signals are required. By combining signal amplification, filtering, and standardized output conversion in a single device, the EMS170 enables the integration of strain gauge sensors into both industrial and research measurement setups.

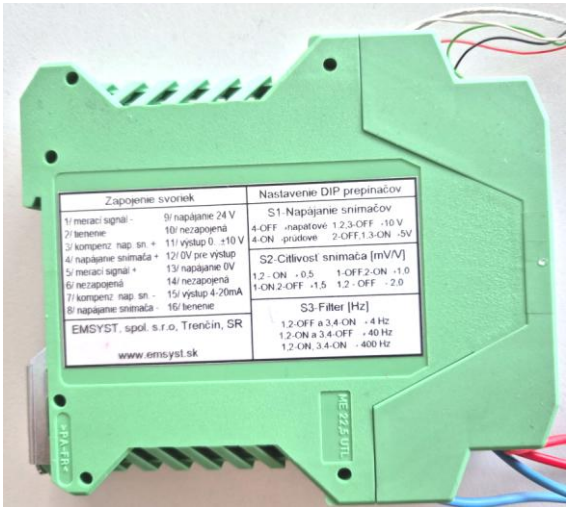

Figure 2. Converter EMS170

3.3 PLC

For the purpose of controlling the position of the linear axis in experiments aimed at determining the stiffness of fluid actuators, a control system based on the Schneider M241CEC programmable logic controller (Fig. 3) was implemented. This solution was chosen for its flexibility, modularity, and the possibility of effective integration into the experimental measurement setup [Duhancik 2024].

The parameterization of the control algorithm allows for precise positioning of the linear axis to the desired reference position at a defined movement speed, ensuring the reproducibility of measurement cycles and enabling adaptive modification of process conditions depending on experimental requirements. The measured signal is processed by an analog input module designed to acquire the output from a strain gauge transducer. This transducer converts the low-level voltage signal from the strain gauge bridges into a standardized analog signal in the range of 0 to 10 V, compatible with the PLC input. The output voltage is linearly proportional to the applied force in the range of 0 to 10 N, which allows for a clear conversion of the voltage level into the physical quantity of force and subsequent numerical processing of the measured data in the control system.

Figure 3. PLC M241CE + Analog modul TM3AI4

Shifting the zero level of the measured signal to 0.044 V (at the upper limit of 10 V) serves, among other things, as a diagnostic element for verifying the integrity of the measuring chain, allowing the identification of any interruption or failure of the electrical signal during the experiment. The non-zero lower limit thus represents a control reference point through which it is possible to distinguish a valid measured signal from an error condition (e.g., power failure or conductor interruption).

Due to the aforementioned shift in the zero level, it was necessary to implement a mathematical correction of the input analog signal, which ensures its accurate transformation into a physical force quantity in the range of 0 to 10 N. The correction algorithm compensates for the signal offset and ensures a linear conversion of the voltage level into the corresponding load value.

The modified signal allows the current value of the force acting on the strain gauge sensor integrated into the linear axis to be clearly determined at any given moment. This force directly represents the system's response to fluid muscle deformation and forms the basis for quantifying its stiffness characteristics.

The software sequence for controlling automated measurements is defined by three basic steps (Fig. 4):

- Initialization
- Measurement execution phase
- Measurement finalization

The measurement begins at the initial position, which is determined as close as possible to the position of the fluid muscle in a resting state to ensure measurement over the longest possible trajectory. Before activating the measurement, it is necessary to define the required extension speed and the final position at which the stiffness of the fluid muscle will be measured.

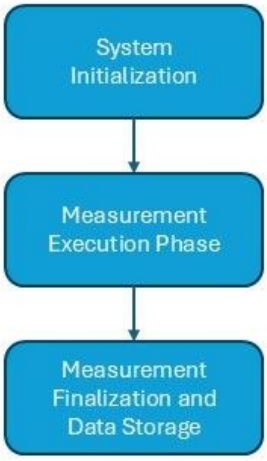

Figure 4. Program flowchart

After reaching the final position, there is a time delay for a defined period, during which the average value of the measured force exerted by the fluid muscle against the measuring apparatus is calculated. This average value is recorded in the memory of the PLC system.

After recording the given value, the extension is automatically returned to the base position. This entire process is repeated a defined number of times in order to obtain a relevant number of measured samples, from which the average value is determined during the evaluation.

3.4 HMI

An important element of the proposed measurement system is the implementation of an application interface for a touchscreen operator panel, which provides human-machine interaction (HMI). For the needs of the experimental workplace, the Schneider Electric HMI STU6400 panel was chosen, as it is compatible with the control system used and enables effective integration within a unified development environment.

The selected configuration was designed to minimize communication delays and ensure reliable data transfer between the PLC and the display interface, mainly thanks to the support of the manufacturer's native communication drivers. This architecture also simplifies the implementation of the visualization application and increases the overall robustness of the system. The operator panel can be used not only to continuously monitor the current values of process variables (axis position, force, measurement status), but also to enter and modify experimental parameters such as target position, movement speed, number of repetitions, and dwell time at the end position (Fig. 5). The parameters defined in this way allow flexible adjustment of measurement conditions and ensure the reproducibility of experimental cycles when evaluating the stiffness characteristics of fluid actuators.

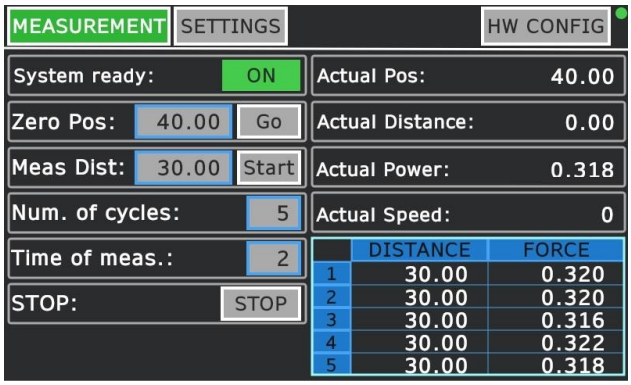

Figure 5. Operator panel

3.5 SMC

In linear drives, an electric motor drives a ball screw or guide mechanism, converting rotary motion into linear motion. Because position, speed, and force can be programmed via a controller, electric drives enable precise and repeatable motion profiles, which are ensured by vector control of electromagnetic flux and torque [Duhancik 2022].

They are widely used in industry in automated assembly lines, pick-and-place systems, pressing and joining processes, and material handling equipment. Compared to pneumatic systems, electric drives offer higher positioning accuracy and easier integration into PLC-based control systems. In scientific research, they are commonly used in test rigs, material testing systems, and laboratory automation, where controlled displacement and reproducible load conditions are required.

The SMC LEYG40LEC-150C-R3C918 (Fig. 6) is a rod-type electric linear actuator with integrated guide rods for increased rigidity. It provides a stroke of 150 mm and thrust forces of up to approximately 1 kN, with a positioning repeatability of ±0.02 mm. The actuator is powered by a 24 V DC motor and controlled by a dedicated controller that allows for programmable motion and operation at multiple positions.

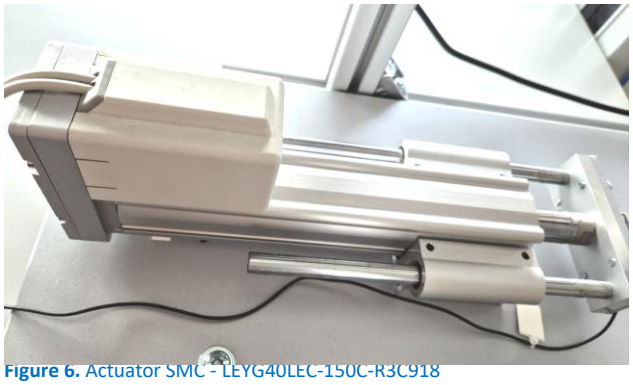

Figure 6. Actuator SMC - LEYG40LEC-150C-R3C918

In practice, this drive is used in automated assembly stations, component insertion and pressing applications, and precision positioning tasks. It is used in automotive production lines, electronics manufacturing systems, packaging machines, and laboratory testing equipment that require precise and stable linear motion [Kondrat 2025].

4 RESULTS

After connection, it was necessary to calibrate the KD34S-10N sensor in order to obtain the actual values of the applied forces in newtons. For this reason, equation (1) was entered into the PLC program, the accuracy of which was verified using calibration weights. After calibrating the sensor in this way, we were ready to start measuring.

$$F_N=(iF_n-C_{sig})*C_{Gacc} \quad (1)$$

where: F_N – resulting force,
iF_N - input measured signal,
C_{sig} – input signal correction,
C_{Gacc} – correction coefficient for conversion to current force.

The measurements were performed in two states. In the first state, the muscle was at rest with 0% vacuum (unloaded). The second state was active, with 95% vacuum (loaded). Subsequently, five measurements were performed at three different extension lengths for each state.

The first measurement was performed with an actuator extension length of 30 mm, the second with a length of 60 mm, and the third with a length of 90 mm. For each measurement, we focused on the forces acting at the end positions (Fig. 7).

Figure 7. Measurement of force in final position

For this reason, the actuator motion program was designed so that, after reaching a certain position, it remained in that position for 2 seconds and then, after the forces had stabilized, the value was recorded in the final table. The values were obtained and recorded in newtons (N).

The measured values in the no-load state can be seen in Tab. 1. From these values, the average for each measured distance was then calculated, and a graph was created to compare the trends and deviations between the individual measurements.

Table 1. Table of values without load - 0% vacuum

Vacuum [%]			0
Distance [mm]	30	60	90
1.	0.320 [N]	0.587 [N]	0.741 [N]
2.	0.320 [N]	0.581 [N]	0.768 [N]
3.	0.316 [N]	0.581 [N]	0.755 [N]
4.	0.322 [N]	0.579 [N]	0.730 [N]
5.	0.318 [N]	0.581 [N]	0.753 [N]
Average	0.319 [N]	0.582 [N]	0.749 [N]

The measured values under load can be seen in Tab. 2. From these values, the average for each measured distance was then calculated and a graph was compiled to compare the course and deviations between individual measurements.

Table 2. Table of values with load – 95% vacuum

Vacuum [%]			95
Distance [mm]	30	60	90
1.	0.867 [N]	1.577 [N]	2.037 [N]
2.	0.894 [N]	1.656 [N]	2.055 [N]
3.	0.919 [N]	1.776 [N]	2.165 [N]
4.	0.886 [N]	1.587 [N]	2.209 [N]
5.	0.952 [N]	1.660 [N]	2.178 [N]
Average	0.904 [N]	1.651 [N]	2.129 [N]

As mentioned above, the average was calculated for each measured distance, and a table was then created from these values, as shown below (Tab. 3).

Table 3. Table comparing measurement averages

Comparison of averages			
Distance [mm]	30	60	90
Vacuum – 0%	0.319 [N]	0.582 [N]	0.749 [N]
Vacuum – 95%	0.904 [N]	1.651 [N]	2.129 [N]

5 DISCUSSION

The tables above (Tab. 1–3) were used to create graphs, which we will describe in more detail. Let us start with Table 1 – the no-load condition, where no vacuum was created in the muscle, and therefore the muscle acted on the strain gauge sensor only through its own weight and the resulting gravitational force.

As shown in Fig. 8, at a measured distance of 30 mm, the deviations between the results were very small, with an average of 0.319 N and a total range from the smallest measured value to the largest of 0.006 N, which may represent statistical measurement deviation.

When measuring at a greater distance of 60 mm, the individual deviations were larger, and the range from the smallest to the largest value was 0.008 N, which still does not represent a

significant increase compared to the value obtained at a distance of 30 mm.
When measuring at a distance of 90 mm, the range was 0.038 N, which represents a noticeable increase compared to the previous values. We attribute this result to greater rearrangement of the granules, as the deflection distance is greater and therefore the angle at which the muscle was deflected is also greater. This means that there was greater rearrangement of the granules and, consequently, the stiffness of the fluid muscle changed depending on the granule configuration at that moment.

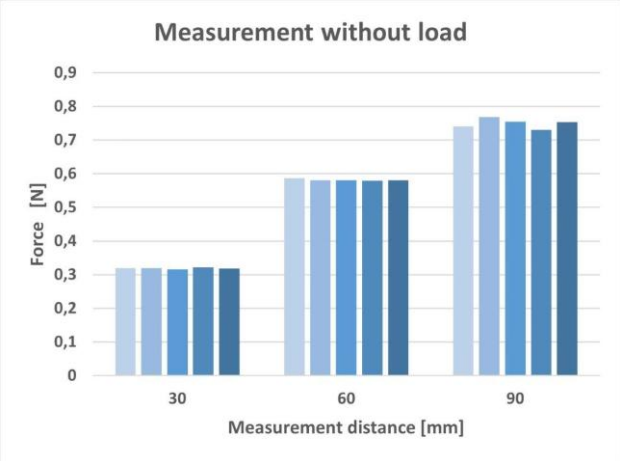

Figure 8. Graph from measurement without load - 0% vacuum

When measuring under load, the curves of the individual measurements can be seen in Fig. 9. As mentioned in the description of the measurement process, after each deflection, the vacuum in the muscle was released so that it could return to its original position. This caused a new rearrangement of the granules in the muscle after each measurement.
It follows that the stiffness changed depending on the mutual arrangement of the granules. As shown in Fig. 9, when measuring at a distance of 30 mm, the values were within a range of 0.085 N. This represents a greater variation compared to the values obtained from the measurement without load, indicating a relatively greater rearrangement of the granules.
When measuring at a distance of 60 mm, this effect is even more noticeable than in the unloaded measurement. The range of the obtained data is 0.193 N, whereas in the measurement without load, the values are essentially constant.
In the final measurement at a distance of 90 mm, the range of values was 0.172 N, which further confirms that after each release of negative pressure and deflection of the muscle to a certain distance, the granules are displaced and rearranged, resulting in a change in the stiffness of the muscle.

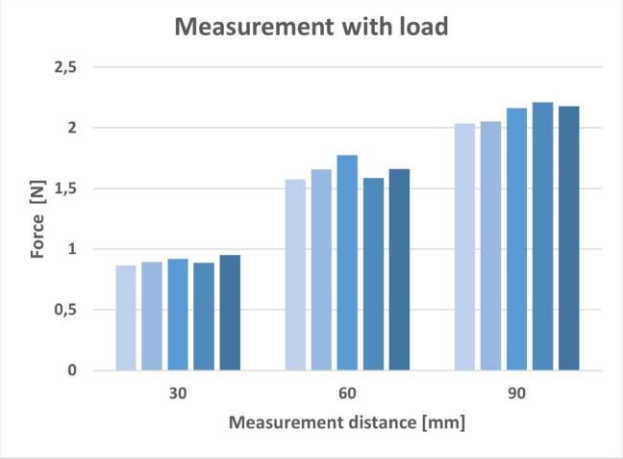

Figure 9. Graph from measurement with load - 95% vacuum

The final graph (Fig. 10) compares the average values obtained from the no-load and load measurements. In both cases, the required force increases with increasing deflection distance, indicating progressive mechanical resistance of the pneumatic muscle.
When the muscle is subjected to additional load, significantly higher forces are required to achieve the same deformation. Overall, the graph shows that both the deflection distance and the vacuum level at which the muscle operates significantly affect the force response of the pneumatic muscle.
The presence of negative pressure significantly increases the force required to achieve the same displacement, reflecting higher effective stiffness under working conditions.
Compared to the measurement without load, the increase in values under load is substantially greater and does not follow the same approximately linear trend observed in the values obtained from the measurement without load.

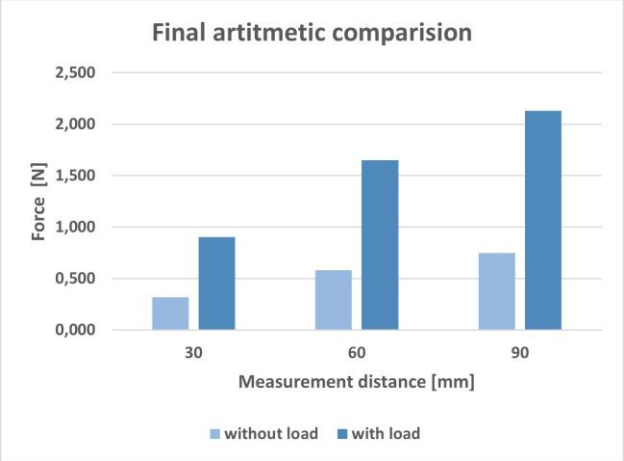

Figure 10. Graph comparing measurement averages

6 CONCLUSION

These results may contribute to research on the stiffness of fluid muscles depending on vacuum pressure and granulate behavior. The proposed approach to measuring the stiffness of fluid muscles addresses one of the key challenges in soft actuation research, namely how to reliably and reproducibly characterize mechanical behavior in highly compliant nonlinear systems. The presented methodology represents an important step towards more standardized evaluation and better comparability between different drive designs.
For future work, we consider it important to extend the focus beyond measuring only the end forces required to deflect the muscle to a given position. In addition to these end force values, capturing the entire force-displacement curve over the full range of motion would provide much deeper insight into mechanical behavior, nonlinearities, hysteresis effects, and potential instability during actuation. Understanding the complete force curve during muscle deflection will greatly improve characterization and control strategies.
Another key direction for future research should be the systematic comparison of experimentally measured stiffness results with model simulations. Aligning real measurements with predictive models will help validate assumptions, improve simulation parameters, and ultimately enable more accurate optimization of the design and control of soft robotic fluid muscles.

ACKNOWLEDGMENTS

This work was supported by the Slovak Research and Development Agency under the contract No. APVV-23-0591, and by the projects VEGA 1/0700/24, KEGA 063TUKE-4/2025 granted by the Ministry of Education, Science, Research, and Sport of the Slovak Republic, and by the EU NextGenerationEU through the Recovery and Resilience Plan for Slovakia under the project No. 09I03-03-V03-00075.

REFERENCES

[Armanini 2022] Armanini, C., et al. Soft Robots Modeling: A Structured Overview. IEEE Transactions on Robotics, 2022, Vol. 39, No. 3, pp. 1729-1748. DOI: 10.1109/TRO.2022.3231360

[Chi 2022] Chi, Y., et al. Bistable and Multistable Actuators for Soft Robots: Structures, Materials, and Functionalities. Advanced Materials, 2022, Vol. 34, No. 19, pp. 1-44. DOI: 10.1002/adma.202110384

[Duhancik 2022] Duhancik, M., et al. Sensorless Control Analysis of Electric Motor Drives Based on High-Frequency Signal Injection and Its Simulation Verification. Actuators, 2022, Vol. 11, No. 11. DOI: 10.3390/act11110317

[Duhancik 2024] Duhancik, M., et al. The Automated Quality Control of 3D Printing Using Technical SMART Device. In: 25th Int. Carpathian Control Conf. (ICCC 2024). DOI: 10.1109/ICCC62069.2024.10569677

[Ebrahimi 2020] Ebrahimi, N., et al. Magnetic Actuation Methods in Bio/Soft Robotics. Advanced Functional Materials, 2020, Vol. 31, No. 11, pp. 1-40. DOI: 10.1002/adfm.202005137

[EMSYST 2025] Emsyst. EMS170. Available at: https://www.emsyst.sk/en/products/electronic-units-and-signal-conditioners/EMS170

[Gulcan 2021] Gulcan, O., et al. The State of the Art of Material Jetting-A Critical Review. Polymers, 2021, Vol. 13, No. 16., pp. 1-19. DOI: 10.3390/polym13162829

[Hasan 2024] Hasan, K., et al. Oceanic Challenges to Technological Solutions: A Review of Autonomous Underwater Vehicle Path Technologies in Biomimicry, Control, Navigation, and Sensing. IEEE Access, 2024, Vol. 12, pp. 46202-46231. DOI: 10.1109/ACCESS.2024.3380458

[Jubelin 2022] Jubelin, C., et al. Three-dimensional in vitro culture models in oncology research. Cell Biosci, 2022, Vol. 12, No. 155, pp. 1-28. DOI: 10.1186/s13578-022-00887-3

[Kondrat 2025] Kondrat, M., et al. Experimental System for Measuring the Bending Stiffness of Soft Actuators Based on Servo Drives. MM Science Journal, 2025, No October, pp. 8686-8691. DOI: 10.17973/MMSJ.2025_10_2025045

[Krushynska 2023] Krushynska, O.A., et al. Emerging topics in nanophononics and elastic, acoustic, and mechanical metamaterials: an overview. Nanophotonics, 2023, Vol. 12, No. 4, pp. 659-686. DOI: 10.1515/nanoph-2022-0671

[Manikantan 2020] Manikantan, H., et al. Surfactant dynamics: hidden variables controlling fluid flows. Journal of Fluid Mechanics, 2020, 892. DOI: 10.1017/jfm.2020.170

[MeSystems 2026] MeSystems. KD34s 500mN. Available at: https://www.me-systeme.de/de/kd34s-500mn

[Mohd Nurazzi 2021] Mohd Nurazzi, N., et al. Fabrication, Functionalization, and Application of Carbon Nanotube-Reinforced Polaymer Composite: An Overview. Polymers, 2021, Vol. 13, No. 7, pp. 1-44. DOI: 10.3390/polym13071047

[Navas 2021] Navas, E., et al. Soft Grippers for automatic Crop Harvesting: A Review. Sensors, 2021, Vol. 21, No. 8, pp. 1-27. DOI: 10.3390/s21082689

[Russo 2023] Russo, M., et al. Continuum Robots: An Overview. Advanced Intelligent Systems, 2023, Vol. 5, No. 5, pp. 1-25. DOI: 10.1002/aisy.202200367

[Schneider 2021] Schneider, J.B., et al. Management of Immune-Related Adverse in Patients Treated With Immune Checkpoint Inhibitor Therapy: ASCO Guideline Update. Journal of Clinical Oncology, 2021, Vol. 39, No. 36, pp. 4073-4126. DOI: 10.1200/JCO.21.01440

[Xavier 2022] Xavier, M.S., et al. Soft Pneumatic Actuators: A review of Design, Fabrication, Modeling, Sensing, Control and Applications. IEEE Access, 2022, Vol. 10, pp. 59442-59485. DOI: 0.1109/ACCESS.2022.3179589

[Yang 2019] Yang, C.J., et al. Electronic Skin: Recent Progress and Future Prospects for Skin-Attachable Devices for Health Monitoring, Robotics, and Prosthetics. Advanced Material, 2019, Vol. 31, No. 48, pp. 1-50. DOI: 10.1002/adma.201904765

[Yang 2021] Yang, Y., et al. Optical trapping with structured light: a review. Advanced Photonics, 2021, Vol. 3, No. 3, pp. 1-40. DOI: 10.1117/1.AP.3.3.034001

[Zidek 2024] Zidek, K., et al. Real-Time Material Flow Monitoring In SMART Automated Lines Using a 3D Digital Shadow with the Industry 4.0 Concept. In: 25th Int. Carpathian Control Conf. (ICCC 2024). DOI: 10.1109/ICCC62069.2024.10569500

CONTACTS:

Assist. Prof. Michal Duhancik
Ing. Martin Kondrat
Assoc. Prof. Kamil Zidek
Prof. Alexander Hosovsky
Prof. Jan Pitel
Assoc. Prof. Tibor Krenicky
Assoc. Prof. Jozef Husar
Technical University of Kosice, Faculty of Manufacturing technologies with the seat in Presov, Bayerova 1, 080 01 Presov, Slovakia
michal.duhancik@tuke.sk; martin.kondrat@tuke.sk; kamil.zidek@tuke.sk; alexander.hosovsky@tuke.sk; jan.pitel@tuke.sk; tibor.krenicky@tuke.sk; jozef.husar@tuke.sk

LICENSE CREATIVE COMMONS: